



PCCP

**Dynamic atomic contributions to infrared intensities of fundamental bands**

Journal:	<i>Physical Chemistry Chemical Physics</i>
Manuscript ID	CP-ART-08-2015-004949.R2
Article Type:	Paper
Date Submitted by the Author:	13-Oct-2015
Complete List of Authors:	da Silva Filho, Arnaldo; Instituto de Química, Richter, Wagner; Instituto de Química, Bassi, Adalberto; Unicamp, Chemistry Department Bruns, Roy; Universidade Estadual de Campinas, Instituto de Química

SCHOLARONE™  
Manuscripts

## Dynamic atomic contributions to infrared intensities of fundamental bands

Arnaldo F. Silva<sup>†</sup>, Wagner E. Richter<sup>†</sup>, Adalberto B. M. S. Bassi<sup>†</sup>, Roy E. Bruns<sup>†</sup>

<sup>†</sup> – Instituto de Química, Universidade Estadual de Campinas, CP 6154, Campinas–SP, Brazil. CEP 13.083-970.

Corresponding author:

Prof. Dr. Roy Edward Bruns  
Instituto de Química, Universidade Estadual de Campinas  
Campinas, São Paulo, Brazil. CEP 13.083–970.  
bruns@iqm.unicamp.br

## Abstract

Dynamic atomic intensity contributions to fundamental infrared intensities are defined as the scalar products of dipole moment derivative vectors for atomic displacements on the total dipole derivative vector of the normal mode. Intensities of functional group vibrations of the fluorochloromethanes can be estimated within  $6.5 \text{ km mol}^{-1}$  by displacing only the functional group atoms rather than all the atoms in the molecules. The asymmetric  $\text{CF}_2$  stretching intensity, calculated to be  $126.5 \text{ km mol}^{-1}$  higher than the symmetric one, is accounted for by an  $81.7 \text{ km mol}^{-1}$  difference owing to the carbon atom displacement and  $40.6 \text{ km mol}^{-1}$  for both fluorine displacements. Within the Quantum Theory of Atoms in Molecules (QTAIM) model differences in atomic polarizations are found to be the most important for explaining the difference in these carbon dynamic intensity contributions. Carbon atom displacements almost completely account for the differences in the symmetric and asymmetric  $\text{CCl}_2$  stretching intensities of dichloromethane, 103.9 of the total calculated value of  $105.2 \text{ km mol}^{-1}$ . Contrary to that found for the  $\text{CF}_2$  vibrations intramolecular charge transfer provoked by the carbon atom displacement almost exclusively explains this difference. The very similar intensity values of the symmetric and asymmetric  $\text{CH}_2$  stretching intensities in  $\text{CH}_2\text{F}_2$  arise from nearly equal carbon and hydrogen atom contributions for these vibrations. All atomic contributions to the intensities for these vibrations in  $\text{CH}_2\text{Cl}_2$  are very small. Sums of dynamic contributions of the individual intensities for all vibrational modes of the molecule are shown to be equal to mass weighted atomic effective charges that can be determined from atomic polar tensors evaluated from experimental infrared intensities and frequencies. Dynamic contributions for individual intensities can also be determined solely from experimental data.

## Introduction

Infrared intensities have been historically studied in spectroscopy mainly for extracting information about molecular electronic structures. Atomic charges, in particular, were widely used by vibrational spectroscopy researchers in many attempts to establish their relations with variations in molecular electronic structure. Many different partition models were developed over the years in order to extract charge information from the infrared spectrum, usually separating infrared intensities into dynamic and static contributions. Sorted by their formulation dates, some of the most successful include Equilibrium Charge–Charge Flux (ECCF)<sup>1</sup>, the Charge–Charge Flux–Overlap (CCFO)<sup>2</sup>, the Charge–Charge Flux–Overlap Modified (CCFOM)<sup>3</sup> and the Charge–Charge Flux–Dipole Flux (CCDFD)<sup>4</sup> model, developed within the physics of Bader's Quantum Theory of Atoms in Molecules (QTAIM)<sup>5</sup>. Recently intensity results were expressed as a squared function of charge, charge flux and dipole flux terms<sup>6</sup>. Furthermore the analysis of the infrared intensities of hydrocarbons has led to a new interpretation of the CCDFD contributions in terms of intramolecular atomic charge transfer and counter polarization. The infrared intensities of the simple hydrocarbons containing  $sp^2$  and  $sp^3$  carbons were quantitatively accounted for by these contributions without the necessity of including a pure charge term. Among the hydrocarbons, the charge contribution is significant only for vibrations with  $sp$  carbons<sup>7</sup>. The CCDFD decomposition was also used to successfully interpret the infrared intensity enhancements of the water dimer<sup>8</sup> and trimer<sup>9</sup> in terms of atomic contributions.

As such this work on the halomethane intensities has two main objectives. First, a better understanding of dynamic atomic intensity contributions for individual vibrations is sought and their potential usefulness for electronic structure analysis is determined by examining atomic parameters for this family of molecules ranging from the nonpolar methane to the very polar fluoro- and chlorofluoromethanes. Second, the sum of these atomic contributions over all the molecular fundamental modes provides an expression for the intensity sum analogous to Crawford's G sum rule<sup>10</sup>. The relation of these dynamic atomic intensity sum contributions with the parameters of the G sum rule, the atomic effective charges, is also presented. Indeed Person and Kubulat<sup>11,12</sup> have suggested the calculation of atomic contributions previously and showed that the sum of these contributions are related to the atomic effective charges of the water molecule. The use of QTAIM leads to an interpretation of the infrared atomic effective charges and the closely related mean dipole moment derivatives, sometimes called GAPT charges<sup>13</sup>, in terms of well-defined electronic structure changes. Furthermore the atomic effective charges can also be evaluated from atomic polar tensors and are linearly related to the electronegativity of a substituent atom whereas the carbon atomic effective charges are related to the average

electronegativity of their substituents<sup>14</sup>. Here the dependence of the dynamic atomic intensity sum contributions on electronegativity is also investigated.

## Calculations and Methodology

### Computational details

The first step of our work was to choose which experimental infrared intensities would be used as references, since there are several measurements from different research groups. Therefore three criteria were used to select the experimental data that would be used: 1) the intensities must have been measured for all the fundamental bands of the molecule, 2) error estimates from scattering of Beer's law plots must have been reported and 3) in the case of hydrogen-containing molecules, intensity measurements and error estimates must have been made for at least two isotopomers. For the fluoro- and chloromethanes isotopomeric intensity data permits some validation of the quality of measured values by means of the G intensity sum rule<sup>10</sup> and the isotopic invariance property of atomic polar tensor elements<sup>15,16</sup>.

The methane data were taken from four different experimental studies<sup>17,18,19,20</sup>. The methyl fluoride data are from Overend and coworkers<sup>21</sup>, methylene fluoride from Kondo *et al.*<sup>22</sup> and fluoroform from Kim and King<sup>23</sup>. The tetrafluoromethane intensities used here are averages of results obtained by three research groups<sup>24,25,26</sup>. The methyl chloride values are averages of results from Russell *et al.*<sup>21</sup>, Dickson *et al.*<sup>27</sup> and Saeki and associates<sup>28</sup>. The methylene chloride results are from Saeki and Tanabe<sup>29</sup> whereas the chloroform data are averages of results from two research groups<sup>30,31</sup>. For carbon tetrachloride results were taken from ref.<sup>32</sup>. Average values from several references were taken for  $\text{CF}_3\text{Cl}$ <sup>33,34</sup>,  $\text{CF}_2\text{Cl}_2$ <sup>35,36,37</sup> and  $\text{CFCl}_3$ <sup>34,35,38,39,40</sup>. Comparisons of theoretical values calculated at the QCISD/cc-pVTZ level with their experimental values resulted in rms errors of 14.8, 22.4 and 22.2  $\text{km mol}^{-1}$  respectively for the fluoro-, chloro- and fluorochloromethanes. This can be considered excellent agreement as the intensity values for these molecules range from almost zero to 414  $\text{km mol}^{-1}$ .

The molecular geometries were optimized using Gaussian03 program<sup>41</sup> on a 64 Opteron workstation which also generated the wave functions to be used by the MORPHY98 program<sup>42</sup>. The optimized geometries were then used to obtain the fundamental infrared intensities and polar tensors also using Gaussian03. The QTAIM multipoles were calculated through MORPHY98 by integrating the equilibrium and distorted wave functions generated by Gaussian03. As in our previous work<sup>43</sup> refined carbon parameters from MORPHY98 were corrected using the multipole moments of the terminal atoms, charge sum neutrality and the molecular dipole moment expression. Distorted geometries were generated by displacing each

atom by 0.01 Å along each Cartesian axis in both the positive and negative directions. Each one of the 6N (N being the number of atoms) distorted geometries and the equilibrium geometry has its own set of AIM atomic multipoles. As will be demonstrated later accurate intensity values can be obtained by displacing only the characteristic group of atoms. The atomic charges and atomic dipoles are then used by the PLACZEK<sup>44</sup> program to calculate the molecular dipole moment derivatives and atomic polar tensors.

## Methodology

The molecular polar tensor<sup>15,16</sup>

$$\mathbf{P}_X = [\mathbf{P}_X^{(1)} : \mathbf{P}_X^{(2)} : \dots : \mathbf{P}_X^{(N)}] \quad (1)$$

is a juxtaposition of 3x3 atomic polar tensors having  $\frac{\partial p_\sigma}{\partial v_j}$  elements where  $\sigma, \nu = x, y, z$ ,  $j=1, \dots, N$ , and N is the number of atoms in the molecule. As the polar tensor elements depend on the molecular orientation in the Cartesian coordinate system, roto-translational invariant polar tensor quantities have been used for the interpretation of polar tensor results in terms of molecular electronic structure. The mean dipole moment derivative, for  $j=1, \dots, N$ ,

$$\bar{p}^{(j)} = \frac{1}{3} \text{Tr}(\mathbf{P}_X^{(j)}) \quad (2)$$

and the closely related atomic effective charge

$$\chi_j^2 = \frac{1}{3} \text{Tr}[\mathbf{P}_X^{(j)} \mathbf{P}_X^{(j)\text{T}}] \quad (3)$$

are most often found in the literature. These invariants have been shown to be related to atomic electronegativities<sup>11</sup> and ionization energies of core electrons through Siegbahn's simple potential model<sup>45</sup>. The atomic effective charges are related to the sum of the intensities,  $\Sigma A_k$ , by the G sum rule<sup>10</sup>

$$\sum_{k=1}^{3N-6} A_k + \Omega = K \sum_{j=1}^N \frac{\chi_j^2}{M_j} \quad (4)$$

where  $K$  is a constant,  $\Omega$ , a rotational correction and  $M_j$  the mass of the  $j^{\text{th}}$  atom. As such the molecular intensity sum can be expressed as a sum of atomic terms involving the squares of the dipole moment derivatives with respect to atomic Cartesian coordinates. Here search is carried out to find atomic invariants for individual intensities that might be useful for their interpretation in terms of molecular electronic structure changes during vibrations.

Within the QTAIM model, for  $\sigma, \nu = x, y, z$ , and  $i, j = 1, \dots, N$ , the polar tensor elements are given by

$$\frac{\partial p_\sigma}{\partial v_j} = q_j^0 + \sum_{i=1}^N \sigma_i^0 \frac{\partial q_i}{\partial v_j} + \sum_{i=1}^N \frac{\partial m_{i,\sigma}}{\partial v_j}, \quad \text{for } \sigma = \nu \quad (5)$$

and

$$\frac{\partial p_\sigma}{\partial v_j} = \sum_{i=1}^N \sigma_i^0 \frac{\partial q_i}{\partial v_j} + \sum_{i=1}^N \frac{\partial m_{i,\sigma}}{\partial v_j}, \quad \text{for } \sigma \neq \nu \quad (6)$$

where  $q_j^0$  is the equilibrium atomic charge on the displaced  $j^{\text{th}}$  atom and  $\sigma_i^0$  is the equilibrium atomic coordinate. The second term of Eq. 5 and first term of Eq. 6 involve atomic charge rearrangements and the last terms correspond to changes in the atomic dipoles of all the atoms owing to this displacement. As such the polar tensor elements contain dynamic atomic contributions to the atomic dipole moment derivatives. On transforming to normal coordinates, for  $k=1, \dots, 3N-6$ ,  $\sigma = x, y, z$ ,

$$\frac{\partial p_\sigma}{\partial Q_k} = \sum_{j=1}^N \left[ \sum_{\nu=x,y,z} \left( \frac{\partial p_\sigma}{\partial v_j} \right) \left( \frac{\partial v_j}{\partial Q_k} \right) \right] = \sum_{j=1}^N \left( \frac{\partial p_\sigma}{\partial Q_k} \right)^{(j)} \quad (7)$$

where Cartesian coordinates of the same atom are grouped together in dynamic atomic contributions. As such, for  $\sigma = x, y, z$ ,  $j=1, \dots, N$

$$\left( \frac{\partial p_\sigma}{\partial Q_k} \right)^{(j)} = q_j^0 \left( \frac{\partial v_j}{\partial Q_k} \right) + \sum_{\nu=x,y,z} \left( \sum_{i=1}^N \frac{\partial [q_i + m_{i,\sigma}]}{\partial v_j} \right) \left( \frac{\partial v_j}{\partial Q_k} \right) \quad (8)$$

This derivative includes equilibrium charge, charge transfer and polarization contributions owing to displacement of the  $j^{\text{th}}$  atom in the  $k^{\text{th}}$  normal coordinate. In general, atomic displacements along one of the Cartesian axes can provoke changes in the charge transfer and polarization contributions in all Cartesian directions while it only provides nonzero charge contributions in the direction of the displaced atom. So, the last term describes change

tendencies in charge transfer and polarization related to displacements of the  $j^{\text{th}}$  atom along the three Cartesian directions, each of which is weighted by its importance in the  $k^{\text{th}}$  normal coordinate.

Alternatively, each dynamic atomic contribution can be expressed as contributions from charge movement, charge rearrangement and atomic dipole change contributions,

$$\left(\frac{\partial p_\sigma}{\partial Q_k}\right)^{(j)} = \left(\frac{\partial p_\sigma}{\partial Q_k}\right)_C^{(j)} + \left(\frac{\partial p_\sigma}{\partial Q_k}\right)_{CF}^{(j)} + \left(\frac{\partial p_\sigma}{\partial Q_k}\right)_{DF}^{(j)} \quad (9)$$

The above atomic dipole derivative contributions will be shown to be useful for simplifying interpretations of changes in electronic structures for molecular vibrations.

As the intensity is proportional to the square of dipole moment derivative, summing over all the fundamental vibrational modes of the molecule with dipole moment changes along the  $\sigma$  direction, for  $\sigma=x,y,z$ , results in

$$\sum_{k=1}^{3N-6} A_{k,\sigma} = K \sum_{k=1}^{3N-6} \left(\frac{\partial p_\sigma}{\partial Q_k}\right) \left(\frac{\partial p_\sigma}{\partial Q_k}\right) \quad (10)$$

$$\sum_{k=1}^{3N-6} A_{k,\sigma} = K \sum_{k=1}^{3N-6} \left\{ \sum_{j=1}^N \left[ \sum_{v=x,y,z} \left(\frac{\partial p_\sigma}{\partial v_j}\right) \left(\frac{\partial v_j}{\partial Q_k}\right) \right] \left[ \sum_{v'=x,y,z} \left(\frac{\partial p_\sigma}{\partial v'_j}\right) \left(\frac{\partial v'_j}{\partial Q_k}\right) \right] \right\} \quad (11)$$

This gives the intensity sum owing to dipole moment changes along the  $\sigma$ -axis. The total intensity sum is the sum of these contributions for each Cartesian direction. The sum in Eq. (11) over the remaining six degrees of freedom is the same as the trace of the matrix in Eq. (30) of the paper by Person and Newton<sup>16</sup> giving the rotational correction term of Eq. (4).

Now, the norm of the vector  $\frac{\partial \vec{p}}{\partial Q_k}$  is proportional to the square root of the intensity and it can involve dipole changes in all three Cartesian coordinate directions,

$$\frac{\partial \vec{p}}{\partial Q_k} = \left(\frac{\partial p_x}{\partial Q_k}\right)^{(1)} \vec{i} + \left(\frac{\partial p_y}{\partial Q_k}\right)^{(1)} \vec{j} + \left(\frac{\partial p_z}{\partial Q_k}\right)^{(1)} \vec{k} + \dots + \left(\frac{\partial p_x}{\partial Q_k}\right)^{(N)} \vec{i} + \left(\frac{\partial p_y}{\partial Q_k}\right)^{(N)} \vec{j} + \left(\frac{\partial p_z}{\partial Q_k}\right)^{(N)} \vec{k} \quad (12)$$

Through Eq. (7),

$$A_k = K \left(\frac{\partial \vec{p}}{\partial Q_k}\right) \cdot \left(\frac{\partial \vec{p}}{\partial Q_k}\right) = K \left[ \sum_{j=1}^N \left(\frac{\partial \vec{p}^{(j)}}{\partial Q_k}\right) \cdot \left(\frac{\partial \vec{p}^{(j)}}{\partial Q_k}\right) \right] \quad (13)$$



$$A_k = A_k^{(1)} + A_k^{(2)} + \dots + A_k^{(N)} \quad (14)$$

As such, a dynamic atomic intensity contribution to the fundamental infrared intensity can be defined as the scalar product of the dipole moment derivative vector for an atomic displacement by the total dipole derivative vector of the normal mode. Thus, the intensity of the  $k^{\text{th}}$  normal mode is simply a sum of the scalar products of the dynamic atomic dipole moment derivatives of all atoms in the molecule by the dipole moment derivative of that normal mode. Within QTAIM the directions of the atomic contributions are determined by the sizes of the Cartesian components represented by Eq. (8) in terms of equilibrium charge displacement, charge transfer and dipolar polarization.

Summing over the  $3N-6$  normal coordinates

$$\sum_{k=1}^{3N-6} A_k = \sum_{j=1}^N \left( \sum_{k=1}^{3N-6} \frac{\partial \vec{p}^{(j)}}{\partial Q_k} \right) \cdot \frac{\partial \vec{p}}{\partial Q_k} \quad (15)$$

Now, comparing Eq. (15) with the G-Sum Rule shown in Eq. (4),

$$\sum_{k=1}^{3N-6} \frac{\partial \vec{p}^{(j)}}{\partial Q_k} \cdot \frac{\partial \vec{p}}{\partial Q_k} = K \left( \frac{\chi_j^2}{M_j} \right) \quad (16)$$

As such, for molecules with no permanent dipole moment (for which  $\Omega$  is null), the square of the atomic effective charge weighted by its inverse mass is just the sum over all normal modes of scalar products of the  $j^{\text{th}}$  atomic dipole moment derivative of the normal mode by the total dipole moment derivative vector of that normal mode. For molecules with a permanent dipole moment,  $\Omega$  can be recovered by also summing over the six translational and rotational modes in Eq. (11).

## Results

### Intensity analysis with dynamic atomic contributions

Characteristic group vibrational frequencies have been used for many years in qualitative analysis being useful for understanding similarities in electronic structure changes on vibrational displacements. Although there has been some activity working with characteristic group intensities<sup>46</sup> their use has been limited perhaps owing to the much larger variations observed for their intensities compared with their frequencies values.

Dynamic contributions of the atoms making up the characteristic group can be used to simplify the intensity analysis. The total dipole moment derivative of a molecular vibration is assumed to be adequately estimated by only the dynamic atomic dipole moment derivative contributions of the atoms composing the functional group. Then the important dynamic contributions are analyzed in terms of equilibrium charge displacement, charge transfer and polarization effects. Table 1 contains the dynamic atomic intensity contributions for 67 normal modes of the fluorochloromethanes. Each normal mode is identified by its characteristic group atoms with the type of vibration, stretching or deformation. Included in the last line for each molecule are values for the atomic intensity sum contributions. Figure 1 contains a graph of the functional group dynamic intensity contributions plotted against the total calculated intensities for most of the normal modes in Table 1. All vibrations are included in Figure 1 except for those of CH<sub>4</sub>, CF<sub>4</sub> and CCl<sub>4</sub> as well as half-dozen others with indefinite band assignments. As can be seen in this figure the agreement is excellent. The rms error is 6.2 km mol<sup>-1</sup> compared with an average intensity of 64.2 km mol<sup>-1</sup>.

Their usefulness is demonstrated by analyzing differences in the absorption intensities of symmetric and asymmetric stretching intensities. It has long been known that asymmetric band intensities are larger than symmetric ones. For C-H vibrations of the difluoro- and dichloroethylenes and the fluorochloromethanes the average asymmetric intensity, 26.6 km mol<sup>-1</sup>, is slightly higher than the symmetric one of 20.4 km mol<sup>-1</sup>. This difference is much more pronounced for the C-F stretching vibrations with the asymmetric average, 232.4 km mol<sup>-1</sup>, being almost double the symmetric one, 143.6 km mol<sup>-1</sup>. In addition, the average value for the asymmetric C-Cl stretching vibrations, 166.6 km mol<sup>-1</sup>, is more than four times the average for the symmetric ones, 36.2 km mol<sup>-1</sup>. The C-F and C-Cl averages include data for the X<sub>2</sub>CY (X=F, Cl; Y=O, S) molecules.

Table 2 contains values of the dynamic atomic contributions to the intensities of the symmetric and asymmetric stretching vibrations of the fluoro- and chloromethanes. It is easily seen that the electronic structure changes resulting in the infrared intensities are largely localized in the characteristic functional group. The first five columns with numerical entries in this table contain the dynamic atomic intensity contributions of each atom in the molecule. Atoms not belonging to the vibrational characteristic group have intensity contributions of less than about 5% of the total intensities.

As examples, electronic structure changes corresponding to the symmetric and asymmetric stretching intensities of difluoro- and dichloromethane are explained in detail. As can be seen in Table 2 dynamic contributions from the CF<sub>2</sub> or CCl<sub>2</sub> atoms explain almost all of the total intensity values for the CF and C-Cl stretching modes. For CH<sub>2</sub>F<sub>2</sub>, contributions from carbon and fluorine sum to 227.5 km mol<sup>-1</sup> for the asymmetric stretch compared with a total value of 227.7 km mol<sup>-1</sup>. For the symmetric stretch these contributions are 105.2 km mol<sup>-1</sup>

compared to  $101.2 \text{ km mol}^{-1}$ . So, the difference in the dynamic contributions of the  $\text{CF}_2$  functional group atoms for these two vibrations is  $122.3 \text{ km mol}^{-1}$  compared to the total calculated difference of  $126.5 \text{ km mol}^{-1}$ . Furthermore, the dynamic carbon contribution difference for these vibrations is  $81.7 \text{ km mol}^{-1}$  or 65% of the total intensity difference. The two dynamic fluorine contributions account for  $40.6 \text{ km mol}^{-1}$  or 32% of this difference. The hydrogen contributions explain a remaining 3%. Therefore, analysis of the carbon and fluorine dynamic contributions provides an assessment of the electronic structure origins of a large portion of the intensity difference between the  $\text{CH}_2\text{F}_2$  symmetric and asymmetric  $\text{CF}_2$  stretches. The experimental values show an even larger difference between these intensities, 269.1 and  $60.6 \text{ km mol}^{-1}$  with the asymmetric intensity value being about four times the symmetric one.

The  $\text{CF}_2$  group forms a local plane in the molecule that can be represented as in Figure 2. The dynamic carbon atom contribution of the functional group atoms of the symmetric stretching dipole derivative can be expressed as ( $z_c^0 = 0$ )

$$\frac{\partial p_z}{\partial Q_{sym}} \approx \left\{ q_c^0 + \left( \frac{\partial q_{F_1}}{\partial z_C} \right) R_{CF}^0 \cos\left(\frac{\alpha}{2}\right) + \left( \frac{\partial q_{F_2}}{\partial z_C} \right) R_{CF}^0 \cos\left(\frac{\alpha}{2}\right) + \frac{\partial m_{C,z}}{\partial z_C} + \frac{\partial m_{F_1,z}}{\partial z_C} + \frac{\partial m_{F_2,z}}{\partial z_C} \right\} \frac{\partial z_C}{\partial Q_{sym}}$$

$$\approx [1.314 + (-0.184)(2.554)(0.580) + (-0.184)(2.554)(0.580) + 0.355 - 0.103 - 0.103](0.205)$$

where  $R_{CF}^0$ ,  $\alpha$  and  $q_c^0$  are the equilibrium C-F bond length, F-C-F angle and equilibrium carbon atomic charge, respectively. Hydrogen atom terms of the dynamic carbon contribution have not been specifically detailed in this equation as they are not important in explaining the intensity difference.

The asymmetric stretch is given by a similar expression ( $y_c^0 = 0$ )

$$\frac{\partial p_y}{\partial Q_{asym}} \approx \left\{ q_c^0 - \left( \frac{\partial q_{F_1}}{\partial y_C} \right) R_{CF}^0 \sin\left(\frac{\alpha}{2}\right) + \left( \frac{\partial q_{F_2}}{\partial y_C} \right) R_{CF}^0 \sin\left(\frac{\alpha}{2}\right) + \frac{\partial m_{C,y}}{\partial y_C} + \frac{\partial m_{F_1,y}}{\partial y_C} + \frac{\partial m_{F_2,y}}{\partial y_C} \right\} \frac{\partial y_C}{\partial Q_{asym}}$$

$$\approx [1.314 - (+0.189)(2.554)(0.812) + (-0.189)(2.554)(0.812) + 0.657 + 0.204 + 0.204](0.214)$$

In terms of the charge displacement, charge transfer and counter polarization contributions

$$\frac{\partial p_z}{\partial Q_{sym}} \approx 0.269 - 0.112 + 0.031 = 0.188 \text{ au}$$

And

$$\frac{\partial p_y}{\partial Q_{asym}} \approx 0.281 - 0.168 + 0.228 = 0.341 \text{ au}$$

The results of this simplified CF<sub>2</sub> group model correspond to 34.5 km mol<sup>-1</sup> for the symmetric and 113.4 km mol<sup>-1</sup> for the asymmetric stretch. Their difference of 78.9 km mol<sup>-1</sup> is close to the difference in the dynamic atomic carbon atom contributions of 81.7 km mol<sup>-1</sup> in Table 2 for these vibrations. The small difference can be attributed to the effects of charge transfer and polarizations of the hydrogen atoms as the carbon atom is displaced.

The charge displacement contributions are almost the same for both normal coordinate derivatives. The negative charge transfer contribution has a somewhat larger magnitude for the asymmetric stretch than the symmetric one even though the magnitudes of the charge derivatives are almost the same. The origin of this difference owes to the larger distance of the charge transfer along y for the asymmetric stretch compared with the one along z for the symmetric stretch owing to F-C-F angle which greater than 90°. The charge transfer contribution is of opposite sign to the counter polarization term as found for most vibrations. The largest difference occurs for the counter polarization. Although the charge transfer term for the asymmetric stretch tends to decrease the dipole moment derivative more than for the symmetric stretch it is more than compensated by the counter polarization term that is about seven times larger for the asymmetric stretch relative to the symmetric one.

These functional group dipole moment derivative contributions are shown in Figure 2. The charge contribution vectors are parallel to the direction of the displaced carbon atom and are about the same size for these two vibrations. The charge transfer vectors are of opposite direction indicating that the fluorine atoms in the direction of the displaced carbon atom become more negatively charged. Finally, the counter polarization vectors are of opposite sense to the charge transfer ones being very large for the asymmetric stretch and much smaller for the symmetric one.

The calculated asymmetric C-Cl stretching intensity for the CCl<sub>2</sub> group is almost ten times the symmetric one, 117.5 km mol<sup>-1</sup> compared with 12.3 km mol<sup>-1</sup>. The CCl<sub>2</sub> group contributions sum to 13.1 km mol<sup>-1</sup> for the symmetric stretch and 126.5 km mol<sup>-1</sup> for the asymmetric one. Both values accurately estimate the total calculated intensities. Indeed the experimental asymmetric intensity of 95 km mol<sup>-1</sup> is even more than ten times the experimental symmetric intensity value of 8.0 km mol<sup>-1</sup>.

The charge displacement, charge transfer and counter polarization contributions for these vibrations are

$$\frac{\partial p_z}{\partial Q_{sym}} \approx 0.058 + 0.065 - 0.016 = 0.107 \text{ au}$$

and

$$\frac{\partial p_y}{\partial Q_{asym}} \approx 0.058 + 0.275 - 0.040 = 0.293 \text{ au}$$

These values correspond to 11.2 and 83.7 km mol<sup>-1</sup> in good agreement with the 10.3 and 103.9 km mol<sup>-1</sup> dynamic carbon intensity contributions in Table 1. Therefore, the total intensity difference calculated for these vibrations of 105.2 km mol<sup>-1</sup> is largely accounted for by the difference in the dynamic carbon contributions of 93.6 km mol<sup>-1</sup> (See Table 2) of which 72.5 km mol<sup>-1</sup> is estimated from the above equations.

As for the CF<sub>2</sub> vibrations, the charge contributions are the same for both derivatives. The charge transfer contribution clearly dominates the asymmetric stretching contributions being 0.210 au larger than the value for the symmetric one. Contrary to the behavior observed for the CF<sub>2</sub> vibrations the counter polarizations are more similar in magnitude with a difference of just 0.024 au. As shown in Figure 2b this large difference has its origin in the magnitudes of the carbon charge derivatives, 0.22 e for the asymmetric stretch and only 0.08 e for the symmetric stretch, in contrast to what was found for the CF<sub>2</sub> stretches where they are similar, as shown in Figure 2. Interestingly the carbon charge derivatives for the CCl<sub>2</sub> vibrations are opposite the CF<sub>2</sub> ones for both the symmetric and asymmetric stretches.

The calculated CHF<sub>3</sub> asymmetric stretching intensity is 160.8 km mol<sup>-1</sup> greater than the symmetric one compared with a difference of 104.9 km mol<sup>-1</sup> for the carbon dynamic contributions in Table 2. The changes in polarizations for these two stretches are larger than the charge transfer difference and account for 72.1 km mol<sup>-1</sup>. As for the CF<sub>2</sub> vibrations in CH<sub>2</sub>F<sub>2</sub>, the equilibrium charge displacements are about the same for both vibrations. The fluorine dynamic contributions are also important and are 49.2 km mol<sup>-1</sup> larger for the asymmetric stretch.

The carbon dynamic contribution for the asymmetric stretch is 111.7 km mol<sup>-1</sup> larger than the symmetric stretch of CHCl<sub>3</sub> and accounts for most of the 126.6 km mol<sup>-1</sup> difference in the total calculated intensities. This difference is principally due to a charge transfer contribution that is 83.7 km mol<sup>-1</sup> larger for the asymmetric stretch. The equilibrium charge and polarization contributions are much smaller as they were for the CCl<sub>2</sub> stretching vibrations.

The calculated intensities of the symmetric and asymmetric CH<sub>2</sub> stretching vibrations of CH<sub>2</sub>F<sub>2</sub> are almost the same for stretching modes, 43.7 and 40.8 km mol<sup>-1</sup>. The CH<sub>2</sub> functional group contributions are 43.9 and 40.8 km mol<sup>-1</sup>, respectively, in excellent agreement with the theoretical values. This compares with experimental values of 26.7 and 41.6 km mol<sup>-1</sup>.

The carbon and hydrogen dynamic contributions are almost the same for these stretching motions. The symmetric stretching intensity is a little higher than the asymmetric one owing to its slightly larger hydrogen dynamic contribution,  $15.1 \text{ km mol}^{-1}$  for each hydrogen, compared with  $13.1 \text{ km mol}^{-1}$ . The carbon contributions are about the same,  $13.7$  and  $14.6 \text{ km mol}^{-1}$ , the smaller value corresponding to the symmetric stretch. Decomposition of these values shows that the individual charge, charge transfer and polarization contributions are also very similar for both vibrations.

The experimental and calculated intensities for the  $\text{CH}_2$  stretching vibrations are in good agreement for  $\text{CH}_2\text{Cl}_2$ . For the symmetric mode, these values are  $6.9$  and  $8.1 \text{ km mol}^{-1}$ , respectively, and for the asymmetric one,  $0.0$  and  $0.1 \text{ km mol}^{-1}$ . This difference for the calculated intensities is accounted for by carbon and hydrogen atom contributions of  $2.3$  and  $2.9 \text{ km mol}^{-1}$ , respectively, for the symmetric stretch while they are only  $0.1$  and  $0.0 \text{ km mol}^{-1}$  for the asymmetric one.

The above discussion for  $\text{CH}_2\text{F}_2$  and  $\text{CH}_2\text{Cl}_2$  is summarized in Figure 3. The sizes of the atomic contributions are given in bar graphs for all the intensities except the  $\text{CH}_2$  stretches of  $\text{CH}_2\text{Cl}_2$  that are very small. The thin bars below the ones for atomic contributions represent total intensity values.

#### Dynamic atomic contributions to intensity sums

Table 3 contains the atomic contributions to the infrared intensity sums for the fluorochloromethanes. As one can see the contributions for the central carbon atom varies sharply, ranging from  $0.3$  to  $1029.7 \text{ km.mol}^{-1}$ . The highest value is the carbon atom contribution for  $\text{CF}_4$  and the lowest value is found in  $\text{CH}_4$ . It is also worth mentioning that the largest difference between atomic QTAIM charges is also found for  $\text{CF}_4$  (C;  $2.8 \text{ e}$  and F;  $-0.7 \text{ e}$ ), whereas the atomic charges are all close to zero in  $\text{CH}_4$ .

The dynamic atomic intensity sum contributions of terminal atoms do not vary quite as much the carbon atom values. The atomic contributions for the hydrogen atoms range from  $8.5$  to  $26.6 \text{ km.mol}^{-1}$ , the values for the chlorine atoms from  $5.9$  to  $14.7 \text{ km.mol}^{-1}$  and those fluorine from  $42.7$  to  $63.8 \text{ km.mol}^{-1}$ . This observation is consistent with the transferability of polar tensor related parameters for the terminal atoms relative to the carbons in the fluorochloromethanes observed previously by our group<sup>47</sup>. Even though these dynamic atomic contributions for the central carbon atom are not transferable among the fluorochloromethanes as might be expected, they appear to be related to the electronegativities of the terminal atoms bonded to it.

Based on observations of experimental results for polar tensor roto-translational invariants with behaviors similar to those described above, and the fact that the sum of all the fundamental intensities of a molecule can be expressed as a sum of atomic contributions as in

the G-sum rule of Equation 4, an empirical model was proposed 25 years ago for the halomethanes<sup>14</sup>. It contains two basic assumptions: 1) the carbon atom intensity contributions in the halomethanes are proportional to the average electronegativity of the substituent halogen atoms and 2) the halogen atomic intensity contributions are proportional to their own electronegativities.

The first column of Table 3 contains electronegativity model estimates of the carbon contributions for the fluorochloromethanes, determined from only experimental data and the last line has the average values for the terminal atom contributions. The next four columns contain dynamic atomic contributions to the intensity sum determined at the QCISD/cc-pVTZ level.

Figure 4 shows a graph of both the QTAIM and electronegativity model atomic intensity sum contributions against the electronegativities. Minus signs have been assigned to the halogen substituent atoms since they clearly draw electron density from the carbon atoms. The fluoromethane atomic intensity sum contributions from the QCISD/cc-pVTZ QTAIM calculations and the electronegativity model results determined completely from experimental intensity data are in excellent agreement with an rms error of only 20.6 km mol<sup>-1</sup>, or about 2% of the intensity variation. Most of this difference can be attributed to the 14.8 km mol<sup>-1</sup> root mean square difference between the calculated and experimental intensities. The chloro- and fluorochloromethanes show larger deviations from the electronegativity model values, the size of the deviations increasing for carbon atoms with more chlorine substituents. This might have been anticipated as the chlorine atoms are more polarizable than the fluorines that would cause deviations from a model based solely on electronegativity. Furthermore the averages of the QTAIM estimates for hydrogen, fluorine and chlorine atoms are 17.3, 56.5 and 12.0 km.mol<sup>-1</sup>, respectively, in excellent agreement with the 18.1, 56.4 and 8.0 km.mol<sup>-1</sup> obtained using experimental intensity values and assuming transferability of the halogens atoms as done in the electronegativity model.

Fig. 5 shows a graph of the dynamic contributions as a function of mass-weighted squares of effective charges of Eqs. 3 and 4 for all the atoms investigated here. The linear plot is almost perfect and the slope of this line is 2915.2±10.4 km mol<sup>-1</sup> which is the constant used to transform effective charge values in units of  $e^2 amu^{-1}$  to km mol<sup>-1</sup>. The intercept is zero within the estimated error. Experimental values obtained from atomic polar tensors are given in Table 4 along with the QCISD/cc-pVTZ values and are highly correlated. Included in Table 4 are the zero flux equilibrium charges. The difference between the equilibrium charge and the effective charge values is determined by the charge transfer and polarization terms in Eq. 8. As can be seen in Table 4, the sum of the charge transfer and polarization contributions have substantial sizes although the charge contributions are usually much larger. This hinders attempts to obtain accurate atomic charge estimates from infrared intensities.

Zero flux atomic charge values for the carbon atoms in the fluoromethanes are larger than their effective charges whereas they are smaller for the chloromethanes. As might be expected based on this observation, the carbon atomic charge value in  $\text{CCl}_3\text{F}$  is smaller than the effective charge value but it is larger in  $\text{CClF}_3$ . The difference is smaller in  $\text{CCl}_2\text{F}_2$ . As such the sum of the charge transfer and polarization contributions on carbon seems to depend on whether the substituent atom is fluorine or chlorine. The sizes of the fluorine zero flux charges are greater than those of the effective charge showing that the charge transfer and polarization effects partially cancel the charge effect on the intensities. On the other hand, they are smaller for chlorine showing that this sum reinforces the charge effect on the intensities.

## Concluding remarks

Dynamic atomic contributions of both dipole moment derivatives and intensities have already been useful for the interpretation of hydrogen bonding intensity enhancements in the water dimer<sup>8</sup> and trimer<sup>9</sup>. We showed that intensity enhancement on hydrogen bonding for the water dimer can almost be completely accounted for by the intensity contribution of the hydrogen bridge atom. The intensity enhancement by the bridge atom contribution is calculated to be  $145 \text{ km mol}^{-1}$  whereas the total calculated enhancement is almost the same,  $149 \text{ km mol}^{-1}$  (experimental enhancement value of  $141 \text{ km mol}^{-1}$ ). This may be closely connected to the hydrogen bond energy stabilization that has been found to be largely localized in the dimer coulomb and exchange integrals involving the bridge hydrogen and oxygen atoms compared with those integrals in the monomer molecules<sup>48</sup>. As the bridge hydrogen has much greater vibrational amplitude than the oxygen atom for the symmetric stretching mode the corresponding intensity enhancement shows up in the atomic hydrogen intensity contribution. So the bridge hydrogen contribution to the dipole moment derivative seems to be closely related to the hydrogen bonding stabilization energy in the water dimer.

Atomic dipole moment derivative contributions could lead to a fundamental understanding of the correlation between the enthalpies of hydrogen bond formation and the square root of infrared intensity enhancements that have been reported in the literature for many complexes in solution phase<sup>49</sup>. For the water trimer the hydrogen bridge atom contributions account for 99% of the total intensity of the two strongest symmetric stretches. Large portions of the hydrogen bond intensity enhancements in the HF dimer,  $321 \text{ km mol}^{-1}$ , and HF:H<sub>2</sub>O complex,  $592 \text{ km mol}^{-1}$ , are accounted for by the  $237$  and  $576 \text{ km mol}^{-1}$  enhancements calculated for their bridge hydrogen atoms<sup>50</sup>. So these atomic contributions can be expected to simplify the analysis of these enhancements by localizing the regions where the important changes take place.



Dynamic atomic contributions to dipole moment derivatives, defined in Eqs. 7 and 8, should be useful to estimate infrared fundamental intensities. They are vectorial parameters and intensities depend on both their magnitudes and directions. Transference of these atomic derivatives for some terminal atoms could work reasonably well but this will not be adequate for central atoms. Our approach will be to use characteristic substituent shift models<sup>51</sup> proposed by our group sometime ago. This model works accurately for the intensities of the X<sub>2</sub>CY (X=F,Cl,Br; Y=O,S) molecules. The six experimental fundamental intensities of Cl<sub>2</sub>CS were estimated almost within experimental error using only the polar tensors from F<sub>2</sub>CO, Cl<sub>2</sub>CO and F<sub>2</sub>CS determined from experimental intensities<sup>51,52</sup>. In the 2004 reference we have reported 31 characteristic substituent shift relationships for the experimental mean dipole moment derivatives of carbon atoms. Furthermore one can expect many more of these relations to work for carbon atoms as many characteristic shifts have been reported for carbon 1s core ionization energies that are linearly related to carbon mean dipole moment derivatives by Siegbahn's simple potential model<sup>53</sup>.

## Acknowledgements

W.E.R. thanks CNPq (Conselho Nacional de Desenvolvimento Científico e Tecnológico, grant 140711/2013-9) for graduate student fellowship. A.F.S. thanks FAPESP (Fundação de Amparo à Pesquisa do Estado de São Paulo, grant 2014/21241-9) for postdoc research fellowship and R.E.B. thanks CNPq for a research fellowship. We are also grateful to FAPESP (for partial financial support of this work (grant 09/09678-4)).

## References

- <sup>1</sup> J. C. Decius, *J. Mol. Spectrosc.*, 1975, **57**, 384.
- <sup>2</sup> W. T. King and G. B. Mast, *J. Phys. Chem.*, 1976, **80**, 2521.
- <sup>3</sup> M. Gussoni, M. N. Ramos, C. Castiglioni and G. Zerbi, *Chem. Phys. Lett.*, 1987, **142**, 515
- <sup>4</sup> R. L. A. Haiduke and R. E. Bruns, *J. Phys. Chem. A*, 2005, **109**, 2680.
- <sup>5</sup> R. F. W. Bader, *Atoms in Molecules. A Quantum Theory*. Clarendon Press, Oxford, 1990.
- <sup>6</sup> A. F. Silva, W. E. Richter, H. G. C. Meneses, S. H. D. M. Faria, R. E. Bruns. *J. Phys. Chem. A* 116, 8238 (2012)
- <sup>7</sup> A. F. Silva, W. E. Richter, H. G. C. Meneses, R. E. Bruns. *Phys. Chem. Chem. Phys.* 2014, **16** 23224
- <sup>8</sup> A. F. Silva, W. E. Richter, L. A. Terrabuio, R. L. A. Haiduke, R. E. Bruns, *J. Chem. Phys.* 140 084306 (2014)
- <sup>9</sup> A. F. Silva, W. E. Richter, R. E. Bruns, *Chem. Phys. Lett.* 610-611 (2014) 14
- <sup>10</sup> B. L. Crawford, Jr., *J. Chem. Phys.* 20 977 (1952)
- <sup>11</sup> W. B. Person, K. Kubulat, *J. Molecular Struct.* 173 (1988) 357

- 
- <sup>12</sup> W. B. Person, K. Kubulat 224 (1990) 225
- <sup>13</sup> J. Cioslowski, *J. Am. Chem. Soc.* 111 (1989) 8333
- <sup>14</sup> B. B. Neto, R. E. Bruns, *J. Phys. Chem.* 1990 94 1764.
- <sup>15</sup> J. F. Biarge, J. Herranz, J. Morcillo, *An. R. Soc. Esp. Fis. Quim.*, 1961, **A57**, 81.
- <sup>16</sup> Person, W. B.; Newton, J. H. *J. Chem. Phys.* 61 (1974) 1040.
- <sup>17</sup> J. Heicklen, *Spectrochim. Acta A*, 1961, **17**, 201
- <sup>18</sup> J. H. G. Bode, W. M. A. Smit, *J. Phys. Chem.*, 1980, **84**, 198.
- <sup>19</sup> S. Saeki, M. Mizuno, K. Kondo, *Spectrochim. Acta A.*, 1976, **32**, 403.
- <sup>20</sup> K. Kim, *J. Quant. Spectrosc. Radiat. Transfer*, 1987, **37**, 107.
- <sup>21</sup> J. W. Russell, C. D. Needham, J. Overend, *J. Chem. Phys.*, 1966, **45**, 3383.
- <sup>22</sup> S. Kondo, T. Nakanaga, S. Saeki, *J. Chem. Phys.*, 1980, **73**, 5409.
- <sup>23</sup> K. Kim, W. T. King, *J. Chem. Phys.* 1980, **73**, 5591.
- <sup>24</sup> S. Saeki, K. Tanabe, *Spectrochim. Acta A*, 1969, **25**, 1325.
- <sup>25</sup> B. J. Schurin, *Chem. Phys.*, 1959, **30**, 1.
- <sup>26</sup> C. M. Roehl, D. Boglu, G. K. Moortgat, *Geophysical Research Letters*, 1995, **22**, 815.
- <sup>27</sup> A. D. Dickson, I. M. Mills, Jr., B. Crawford, *J. Chem. Phys.*, 1957, **27**, 445.
- <sup>28</sup> S. Kondo, Y. Koga, T. Nakanaga, S. Saeki, *Bull. Chem. Soc. Jpn*, 1983, **56**, 416.
- <sup>29</sup> S. Saeki, K. Tanabe, *Spectrochim. Acta A*, 1969, **25**, 1325.
- <sup>30</sup> K. Tanabe, S. Saeki, *Spectrochim. Acta A*, 1970, **26**, 1469.
- <sup>31</sup> K. Kim, W. T. King, *J. Chem. Phys.*, 1984, **80**, 978.
- <sup>32</sup> K. Tanabe, S. Saeki, *Spectrochim. Acta A*, 1970, **26**, 1469.
- <sup>33</sup> W. B. Person, S. K. Rudys, J. H. Newton, *J. Phys. Chem.*, 1975, **79**, 2525.
- <sup>34</sup> W. G. Golden, D. Horner, J. Overend, *J. Chem. Phys.*, 1978, **68**, 964.
- <sup>35</sup> P. Varanasi, F. K. Ko, *J. Quant. Spectrosc. Radiat. Transfer*, 1977, **17**, 385.
- <sup>36</sup> P. Varanasi, S. Chudmani, *J. Quant. Spectrosc. Radiat. Transfer*, 1988, **39**, 193.
- <sup>37</sup> J. Morcillo, L. J. Zamarano, J. M. V. Heredia, *Spectrochim. Acta A*, 1966, **22**, 1969.
- <sup>38</sup> Z. Li, P. Varanasi, *J. Quant. Spectrosc. Radiat. Transfer*, 1994, **52**, 137.
- <sup>39</sup> R. Names, P. M. Silvaggio, R. W. Boese, *J. Quant. Spectrosc. Radiat. Transfer*, 1980, **23**, 211.
- <sup>40</sup> A. Goldman, F. S. Bonomo, D. G. Murcay, *Ap. Opt.*, 1976, **15**, 2305.
- <sup>41</sup> M. J. Frisch, G. W. Trucks, H. B. Schlegel, G. E. Scuseria, M. A. Robb, J. R. Cheeseman, J. A. Montgomery Jr., T. Vreven, K. N. Kudin, J. C. Burant, J. M. Millam, S. S. Iyengar, J. Tomasi, V. Barone, B. Mennucci, M. Cossi, G. Scalmani, N. Rega, G. A. Petersson, H. Nakatsuji, M. Hada, M. Ehara, K. Toyota, R. Fukuda, J. Hasegawa, M. Ishida, T. Nakajima, Y. Honda, O. Kitao, H. Nakai, M. Klene, X. Li, J. E. Knox, H. P. Hratchian, J. B. Cross, V. Bakken, C. Adamo, J. Jaramillo, R. Gomperts, R. E. Stratmann, O. Yazyev, A. J. Austin, R. Cammi, C. Pomelli, J. W. Ochterski, P. Y. Ayala, K. Morokuma, G. A. Voth, P. Salvador, J. J. Dannenberg, V. G. Zakrzewski, S. Dapprich, A. D. Daniels, M. C. Strain, O. Farkas, D. K. Malick, A. D. Rabuck, K. Raghavachari, J. B. Foresman, J. V. Ortiz, Q. Cui, A. G. Baboul, S. Clifford, J. Cioslowski, B. B. Stefanov, G. Liu, A. Liashenko, P. Piskorz, I. Komaromi, R. L. Martin, D. J. Fox, T. Keith, M. A. Al-Laham, C. Y. Peng, A. Nanayakkara, M. Challacombe, P. M. W.

Gill, B. G. Johnson, W. Chen, M. W. Wong, C. Gonzalez, J. A. Pople. Gaussian 03, Revision D.02. Gaussian, Inc., Wallington CT, 2004.

<sup>42</sup> MORPHY98, a program written by P. L. A. Popelier with a contribution from R. G. A. Bone, UMIST, Manchester, England, EU 1998.

<sup>43</sup> A. F. Silva, J. V. da Silva, Jr., R. L. A. Haiduke, R. E. Bruns. *J. Phys. Chem. A* (2011) 115, 12572.

<sup>44</sup> J. V. da Silva, Jr., L. N. Vidal, P. A. M. Vazquez, R. E. Bruns. *Int. J. Quantum Chem.* (2010) 110, 2029.

<sup>45</sup> P.H. Guadagnini, A. E. Oliveira, R. E. Bruns, B. B. Neto, *J. Am. Chem. Soc.* 1997 119 4224

<sup>46</sup> Hadzi, D, in *Infra-red Spectroscopy and molecular structure*, Davies M. , eds. Elsevier, Amsterdam, 1963

<sup>47</sup> M. N. Ramos, B. Barros Neto, R. E. Bruns. *J. Phys. Chem.* (1985), 89, 4979.

<sup>48</sup> M. Garcia-Revilla, E. Francisco, P. A. Popelier, A. M. Pendás, *ChemPhysChem* (2013), 14, 1211

<sup>49</sup> A. V. Iogansen, *Spectrochim. Acta A* (1999), 55, 1585.

<sup>50</sup> R. L. A. Haiduke, A. E. Oliveira, N. H. Moreira R. E. Bruns *J. Phys. Chem A* (2004), 108, 866

<sup>51</sup> A. B. M. S. Bassi, R. E. Bruns *J. Chem. Phys.* (1975), 82, 3235.

<sup>52</sup> R. E. Bruns *J. Mol. Struct.* (1975), 26, 124.

<sup>53</sup> P. A. Guadagnini, A. E. Oliveira, R. E. Bruns, B. B. Neto *J. Amer. Chem. Soc.* (1997), 119, 4224

Table 1. Dynamic atomic intensity contributions calculated at the QCISD/cc-pVTZ level for the fundamental intensities of the fluorochloromethanes ( $\text{km mol}^{-1}$ ).

Molecule	Vibration		Atomic Contributions					Total
			C(1)	H(2)	H(3)	H(4)	H(5)	
CH <sub>4</sub>			C(1)	H(2)	H(3)	H(4)	H(5)	Total
	v C-H	Q <sub>3</sub>	0.3	1.0	15.5	5.8	0.6	23.2
	v C-H	Q <sub>3</sub>	0.3	6.5	1.4	11.1	3.9	23.2
	v C-H	Q <sub>3</sub>	0.3	10.0	0.2	0.2	12.6	23.3
	δ H-C-H	Q <sub>4</sub>	-0.2	1.7	2.1	3.3	3.3	10.2
	δ H-C-H	Q <sub>4</sub>	-0.2	3.2	3.1	1.2	3.0	10.3
	δ H-C-H	Q <sub>4</sub>	-0.2	3.0	2.7	3.3	1.5	10.3
Total			0.3	25.4	25.0	24.9	24.9	100.5
CH <sub>3</sub> F			C(1)	F(2)	H(3)	H(4)	H(5)	Total
	v C-H	Q <sub>1</sub>	6.7	-0.3	7.3	7.8	7.8	29.3
	δ H-C-H	Q <sub>2</sub>	5.3	-0.8	-0.5	-0.5	-0.5	3.0
	v C-F	Q <sub>3</sub>	59.7	42.3	-0.9	-0.9	-0.9	99.3
	v C-H	Q <sub>4</sub>	6.5	0.0	17.0	3.2	6.4	33.1
	v C-H	Q <sub>4</sub>	6.7	0.0	0.4	15.7	12.4	35.2
	δ H-C-H	Q <sub>5</sub>	-1.2	0.1	1.9	0.9	0.9	2.6
	δ H-C-H	Q <sub>5</sub>	-1.2	0.1	0.5	1.6	1.6	2.6
	---	Q <sub>6</sub>	1.9	0.5	0.0	-0.3	-0.4	1.7
---	Q <sub>6</sub>	1.9	0.5	-0.5	-0.2	-0.1	1.6	
Total			86.3	42.4	25.2	27.3	27.2	208.4
CH <sub>2</sub> F <sub>2</sub>			C(1)	F(2)	F(3)	H(4)	H(5)	Total
	v C-H	Q <sub>1</sub>	13.7	-0.1	-0.1	15.1	15.1	43.7

	$\delta$ H-C-H	Q <sub>2</sub>	3.5	-0.1	-0.1	-1.0	-1.0	1.3
	$\nu$ C-F	Q <sub>3</sub>	69.8	17.7	17.7	-2.0	-2.0	101.2
	$\delta$ F-C-F	Q <sub>4</sub>	8.0	-1.1	-1.1	-0.2	-0.2	5.4
	$\nu$ C-H	Q <sub>6</sub>	14.6	0.0	0.0	13.1	13.1	40.8
	---	Q <sub>7</sub>	17.4	1.6	1.6	0.1	0.1	20.8
	$\delta$ H-C-H	Q <sub>8</sub>	25.3	-0.9	-0.9	-0.1	-0.1	23.3
	$\nu$ C-F	Q <sub>9</sub>	151.5	38.0	38.0	0.1	0.1	227.7
Total			303.8	55.3	55.3	25.1	25.1	464.5
CHF <sub>3</sub>			C(1)	H(2)	F(3)	F(4)	F(5)	Total
	$\nu$ C-H	Q <sub>1</sub>	18.7	16.6	0.0	0.0	0.0	35.3
	$\nu$ C-F	Q <sub>2</sub>	84.6	-6.6	8.7	8.7	8.7	104.1
	$\delta$ F-C-F	Q <sub>3</sub>	17.8	-1.4	-0.6	-0.6	-0.6	14.6
	$\delta$ H-C-F	Q <sub>4</sub>	61.4	-0.1	1.1	1.6	1.5	65.5
	$\delta$ H-C-F	Q <sub>4</sub>	61.3	-0.1	1.7	1.2	1.3	65.4
	$\nu$ C-F	Q <sub>5</sub>	189.5	0.1	1.3	37.8	36.2	264.9
	$\nu$ C-F	Q <sub>5</sub>	189.4	0.1	48.9	12.4	14.0	264.8
	$\delta$ F-C-F	Q <sub>6</sub>	6.8	0.0	-4.9	0.6	0.5	3.0
	$\delta$ F-C-F	Q <sub>6</sub>	6.8	0.0	2.4	-3.1	-3.1	3.0
Total			636.3	8.6	58.6	58.6	58.5	820.6
CF <sub>4</sub>			C(1)	F(2)	F(3)	F(4)	F(5)	Total
	$\nu$ C-F	Q <sub>3</sub>	330.7	3.2	3.2	31.7	38.2	407.0
	$\nu$ C-F	Q <sub>3</sub>	330.2	6.3	35.6	20.2	14.2	406.5
	$\nu$ C-F	Q <sub>3</sub>	330.7	47.8	18.4	5.3	4.8	407.0
	$\delta$ F-C-F	Q <sub>4</sub>	12.7	-9.5	0.9	0.8	0.8	5.7
	$\delta$ F-C-F	Q <sub>4</sub>	12.7	2.2	-8.3	-0.4	-0.4	5.8
	$\delta$ F-C-F	Q <sub>4</sub>	12.7	2.2	2.2	-5.6	-5.6	5.9
Total			1029.7	52.2	52.0	52.0	52.0	1237.9
CH <sub>3</sub> Cl			C(1)	Cl(2)	H(3)	H(4)	H(5)	Total
	$\nu$ C-H	Q <sub>1</sub>	4.1	0.0	6.4	6.4	6.4	23.3
	$\delta$ H-C-H	Q <sub>2</sub>	7.5	-0.5	2.3	2.3	2.3	13.9
	$\nu$ C-Cl	Q <sub>3</sub>	22.7	6.6	-1.7	-1.7	-1.7	24.2
	$\nu$ C-H	Q <sub>4</sub>	0.9	0.0	2.9	0.2	2.0	6.0
	$\nu$ C-H	Q <sub>4</sub>	0.9	0.0	0.5	3.2	1.4	6.0
	$\delta$ H-C-H	Q <sub>5</sub>	-0.6	0.0	4.0	1.0	0.4	4.8
	$\delta$ H-C-H	Q <sub>5</sub>	-0.6	0.0	-0.4	2.6	3.2	4.8
	---	Q <sub>6</sub>	-0.6	-0.2	1.0	0.9	0.9	2.0
	---	Q <sub>6</sub>	-0.6	-0.2	0.9	1.0	0.9	2.0
Total			33.7	5.7	15.9	15.9	15.8	87.0
CH <sub>2</sub> Cl <sub>2</sub>			C(1)	Cl(2)	Cl(3)	H(4)	H(5)	Total
	$\nu$ C-H	Q <sub>1</sub>	2.3	0.0	0.0	2.9	2.9	8.1
	$\delta$ H-C-H	Q <sub>2</sub>	0.0	0.0	0.0	0.0	0.0	0.0
	$\nu$ C-Cl	Q <sub>3</sub>	10.3	1.4	1.4	-0.4	-0.4	12.3
	$\delta$ Cl-C-Cl	Q <sub>4</sub>	0.9	-0.2	-0.2	0.0	0.0	0.5
	$\nu$ C-H	Q <sub>6</sub>	0.1	0.0	0.0	0.0	0.0	0.1

	---	Q <sub>7</sub>	-0.7	-0.1	-0.1	0.9	0.9	0.9
	$\delta$ H-C-H	Q <sub>8</sub>	23.5	-0.9	-0.9	10.3	10.3	42.3
	$\nu$ C-Cl	Q <sub>9</sub>	103.9	11.3	11.3	-4.5	-4.5	117.5
Total			140.3	11.5	11.5	9.2	9.2	181.7
CHCl <sub>3</sub>			C(1)	H(2)	Cl(3)	Cl(4)	Cl(5)	Total
	$\nu$ C-H	Q <sub>1</sub>	-0.1	0.4	0.0	0.0	0.0	0.3
	$\nu$ C-Cl	Q <sub>2</sub>	3.9	0.5	0.3	0.3	0.3	5.3
	$\delta$ Cl-C-Cl	Q <sub>3</sub>	0.5	0.1	-0.1	-0.1	-0.1	0.4
	$\delta$ H-C-Cl	Q <sub>4</sub>	14.3	10.1	-0.7	-0.1	-0.1	23.5
	$\delta$ H-C-Cl	Q <sub>4</sub>	14.3	10.2	0.1	-0.5	-0.5	23.5
	$\nu$ C-Cl	Q <sub>5</sub>	115.6	-5.2	0.4	10.6	10.6	132.0
	$\nu$ C-Cl	Q <sub>5</sub>	115.6	-5.2	14.0	3.8	3.8	131.9
	---	Q <sub>6</sub>	0.8	-0.1	-0.6	0.0	0.0	0.1
	---	Q <sub>6</sub>	0.8	-0.1	0.2	-0.4	-0.4	0.1
Total			265.7	10.7	13.6	13.6	13.6	317.1
CCl <sub>4</sub>			C(1)	Cl(2)	Cl(3)	Cl(4)	Cl(5)	
	$\nu$ C-Cl	Q <sub>3</sub>	119.3	0.4	0.4	7.7	9.6	137.4
	$\nu$ C-Cl	Q <sub>3</sub>	119.3	1.1	9.0	4.9	3.1	137.4
	$\nu$ C-Cl	Q <sub>3</sub>	115.7	12.1	0.6	1.0	0.9	137.4
	$\delta$ Cl-C-Cl	Q <sub>4</sub>	-0.1	0.1	0.0	0.0	0.0	0.0
	$\delta$ Cl-C-Cl	Q <sub>4</sub>	-0.1	0.0	0.1	0.0	0.0	0.0
	$\delta$ Cl-C-Cl	Q <sub>4</sub>	-0.1	0.0	0.0	0.0	0.0	0.0
Total			354.0	13.7	10.1	13.6	13.6	412.2
CCl <sub>3</sub> F			C(1)	F(2)	Cl(3)	Cl(4)	Cl(5)	Total
	$\nu$ C-F	Q <sub>1</sub>	123.9	54.9	0.2	0.2	0.2	179.4
	$\nu$ C-Cl	Q <sub>2</sub>	5.3	-5.0	0.4	0.4	0.4	1.5
	$\delta$ Cl-C-Cl	Q <sub>3</sub>	-0.6	0.6	0.0	0.0	0.0	0.0
	$\nu$ C-Cl	Q <sub>4</sub>	207.1	5.6	0.6	10.5	10.5	234.3
	$\nu$ C-Cl	Q <sub>4</sub>	207.0	5.6	13.7	3.9	3.9	234.1
	$\delta$ F-C-Cl	Q <sub>5</sub>	0.3	0.5	-0.5	-0.1	-0.1	0.1
	$\delta$ F-C-Cl	Q <sub>5</sub>	0.3	0.5	0.0	-0.4	-0.4	0.0
	$\delta$ F-C-Cl	Q <sub>5</sub>	-0.2	0.1	0.1	0.0	0.0	0.0
	$\delta$ F-C-Cl	Q <sub>5</sub>	-0.2	0.1	-0.1	0.1	0.1	0.0
			542.9	62.9	14.4	14.6	14.6	649.4
CCl <sub>2</sub> F <sub>2</sub>			C(1)	F(2)	F(3)	Cl(4)	Cl(5)	Total
	$\nu$ C-F	Q <sub>1</sub>	220.5	35.3	35.3	1.1	1.1	293.3
	$\nu$ C-Cl	Q <sub>2</sub>	0.2	0.5	0.5	-0.5	-0.5	0.2
	$\delta$ Cl-C-Cl	Q <sub>3</sub>	22.2	-6.7	-6.8	1.4	1.4	11.5
	$\delta$ Cl-C-Cl	Q <sub>4</sub>	-0.4	0.2	0.2	0.0	0.0	0.0
	$\nu$ C-F	Q <sub>6</sub>	154.8	28.3	28.3	0.1	0.1	211.6
	$\delta$ F-C-F	Q <sub>7</sub>	0.0	-0.1	-0.1	0.1	0.1	0.0
	$\nu$ C-Cl	Q <sub>8</sub>	335.0	8.4	8.4	11.7	11.7	375.2
	$\delta$ F-C-F	Q <sub>9</sub>	3.6	-1.6	-1.6	0.1	0.1	0.6
Total			735.9	64.3	64.2	14.0	14.0	892.4

CClF <sub>3</sub>			C(1)	Cl(2)	F(3)	F(4)	F(5)	Total
v C-F	Q <sub>1</sub>		384.9	6.3	25.9	27.0	27.0	471.1
v C-Cl	Q <sub>2</sub>		48.8	4.3	-6.3	-6.3	-6.3	34.2
δ F-C-F	Q <sub>3</sub>		0.0	0.1	0.0	0.0	0.0	0.1
v C-F	Q <sub>4</sub>		227.6	0.2	41.7	10.3	13.9	293.7
v C-F	Q <sub>4</sub>		227.9	0.2	2.2	33.7	30.0	294.0
δ F-C-F	Q <sub>5</sub>		7.6	0.1	1.7	-3.4	-3.5	2.5
δ F-C-F	Q <sub>5</sub>		7.5	0.1	-5.2	0.0	0.1	2.5
δ Cl-C-F	Q <sub>6</sub>		0.5	0.0	-0.6	0.1	0.1	0.1
δ Cl-C-F	Q <sub>6</sub>		0.5	0.0	-0.1	-0.2	-0.2	0.0
Total			905.3	11.3	59.3	61.2	61.1	1098.2

Table 2. Dynamic atomic intensity contributions calculated at the QCISD/cc-pVTZ level for the symmetric and asymmetric stretching intensities of the fluorochloromethanes (km mol<sup>-1</sup>).

Molecule	Vibration	Atom (1)	Atom(2)	Atom(3)	Atom(4)	Atom(5)	Total
CH <sub>3</sub> F		(C)	(F)	(H)	(H)	(H)	-
	C-H sym	6.7	-0.3	7.3	7.8	7.8	29.3
	C-H asym	6.5	0.0	17.0	3.2	6.4	33.1
CH <sub>2</sub> F <sub>2</sub>		(C)	(F)	(F)	(H)	(H)	-
	C-H sym	13.7	-0.1	-0.1	15.1	15.1	43.7
	C-H asym	14.6	0.0	0.0	13.1	13.1	40.8
CHF <sub>3</sub>		(C)	(F)	(F)	(H)	(H)	-
	C-F sym	69.8	17.7	17.7	-2.0	-2.0	101.2
	C-F asym	151.5	38.0	38.0	0.1	0.1	227.7
CH <sub>2</sub> Cl <sub>2</sub>		(C)	(Cl)	(Cl)	(H)	(H)	-
	C-H sym	2.3	0.0	0.0	2.9	2.9	8.1
	C-H asym	0.1	0.0	0.0	0.0	0.0	0.1
CHCl <sub>3</sub>		(C)	(Cl)	(Cl)	(H)	(H)	-
	C-Cl sym	10.3	1.4	1.4	-0.4	-0.4	12.3
	C-Cl asym	103.9	11.3	11.3	-4.5	-4.5	117.5
CHCl <sub>3</sub>		(C)	(H)	(Cl)	(Cl)	(Cl)	-
	C-Cl sym	3.9	0.5	0.3	0.3	0.3	5.3
	C-Cl asym	115.6	-5.2	14.0	3.8	3.8	131.9

Table 3. Atomic contributions to the sum of the fundamental infrared intensities of the fluorochloromethanes calculated at the QCISD/cc-pVTZ level and from the electronegativity model.

Molecule	C (Exp)	C	H	Cl	F	Total
----------	---------	---	---	----	---	-------

CH <sub>4</sub>	5.1	0.3	25.1	-	-	100.5
CH <sub>3</sub> F	97.9	86.3	26.6	-	42.7	208.8
CH <sub>2</sub> F <sub>2</sub>	307.1	303.8	25.1	-	55.3	464.5
CHF <sub>3</sub>	632.8	636.3	8.5	-	58.3	820.6
CF <sub>4</sub>	1073.8	1029.7	-	-	51.9	1237.9
CH <sub>3</sub> Cl	31.6	33.7	15.8	5.9	-	87.0
CH <sub>2</sub> Cl <sub>2</sub>	81.1	140.3	9.3	11.5	-	181.7
CHCl <sub>3</sub>	153.1	265.7	10.9	13.6	-	317.1
CCl <sub>4</sub>	246.4	354.0	-	12.9	-	412.2
CCl <sub>3</sub> F	398.3	542.9	-	14.7	62.9	649.4
CCl <sub>2</sub> F <sub>2</sub>	586.5	735.9	-	14.1	63.8	892.4
CClF <sub>3</sub>	811.0	905.3	-	11.4	60.7	1098.2
$\bar{x}$	-	-	17.3	12	56.5	-
Electro. Model	-	-	18.1	8.0	56.4	-

Table 4 . Calculated QTAIM zero flux charges and effective charges at the QCISD/cc-pVTZ level, experimental effective charge values and dynamic atomic contributions for the fluorochloromethanes.

Molecule	Atom	$q_{ZF}$ (e)	$\chi_{\alpha}$ (e)		DAC (km.mol <sup>-1</sup> )
			Experimental	QCISD/	
CH <sub>4</sub>	C	0.013	0.016	0.000	0.1
	H	-0.003	0.054	0.082	24.9
CH <sub>3</sub> F	C	0.650	0.606	0.632	86.2
	H	0.016	0.096	0.100	27.2
	F	-0.699	0.581	0.566	42.6
CH <sub>2</sub> F <sub>2</sub>	C	1.314	1.059	1.156	303.6
	H	0.046	0.079	0.082	25.1
	F	-0.703	0.574	0.603	55.3
CHF <sub>3</sub>	C	2.021	1.546	1.627	635.7
	H	0.091	0.043	0.058	8.17
	F	-0.704	0.591	0.608	58.5
CF <sub>4</sub>	C	2.786	2.051	2.055	1028.7
	F	-0.696	0.547	0.580	52.0
CH <sub>3</sub> Cl	C	0.140	0.363	0.387	33.7
	H	0.044	0.074	0.082	5.9
	Cl	-0.271	0.301	0.306	15.9
CH <sub>2</sub> Cl <sub>2</sub>	C	0.255	0.676	0.772	140.3
	H	0.087	0.052	0.058	9.3
	Cl	-0.214	0.335	0.370	11.6
CHCl <sub>3</sub>	C	0.363	0.940	1.047	265.6
	H	0.124	0.048	0.058	10.4
	Cl	-0.163	0.373	0.396	13.6
CCl <sub>4</sub>	C	0.466	1.043	1.211	357.5

---

CCl <sub>3</sub> F	Cl	-0.117	0.322	0.404	13.7
	C	1.051	1.354	1.492	542.6
	F	-0.680	0.608	0.640	62.8
CCl <sub>2</sub> F <sub>2</sub>	Cl	-0.124	0.428	0.416	14.6
	C	1.636	1.649	1.737	735.4
	F	-0.687	0.661	0.645	64.1
CClF <sub>3</sub>	Cl	-0.131	0.353	0.408	14.0
	C	2.211	2.058	1.928	904.6
	F	-0.692	0.695	0.624	60.7
	Cl	-0.135	0.204	0.361	11.3

---



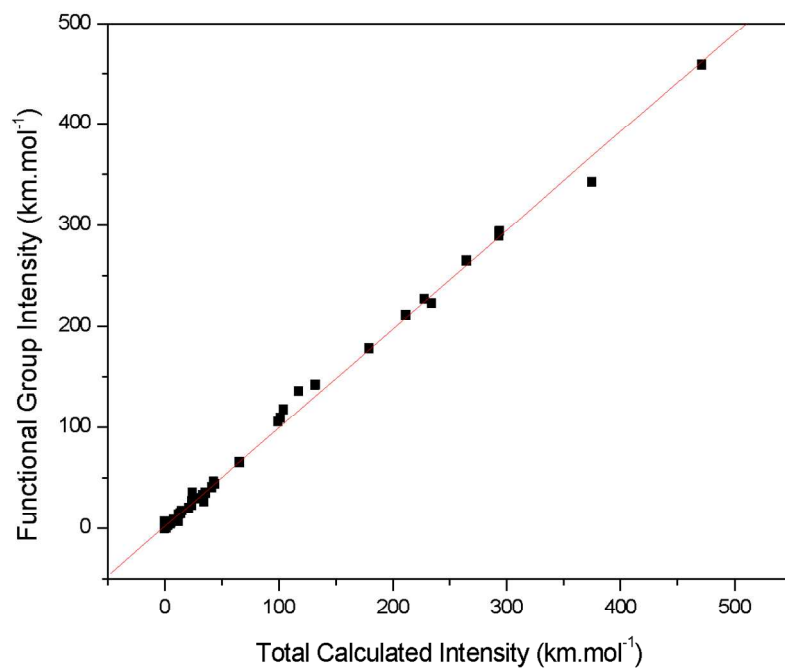


Figure 1. Sums of the dynamic atomic contributions of the functional group atoms vs. the total intensities of the fluorochloromethanes.

279x215mm (150 x 150 DPI)

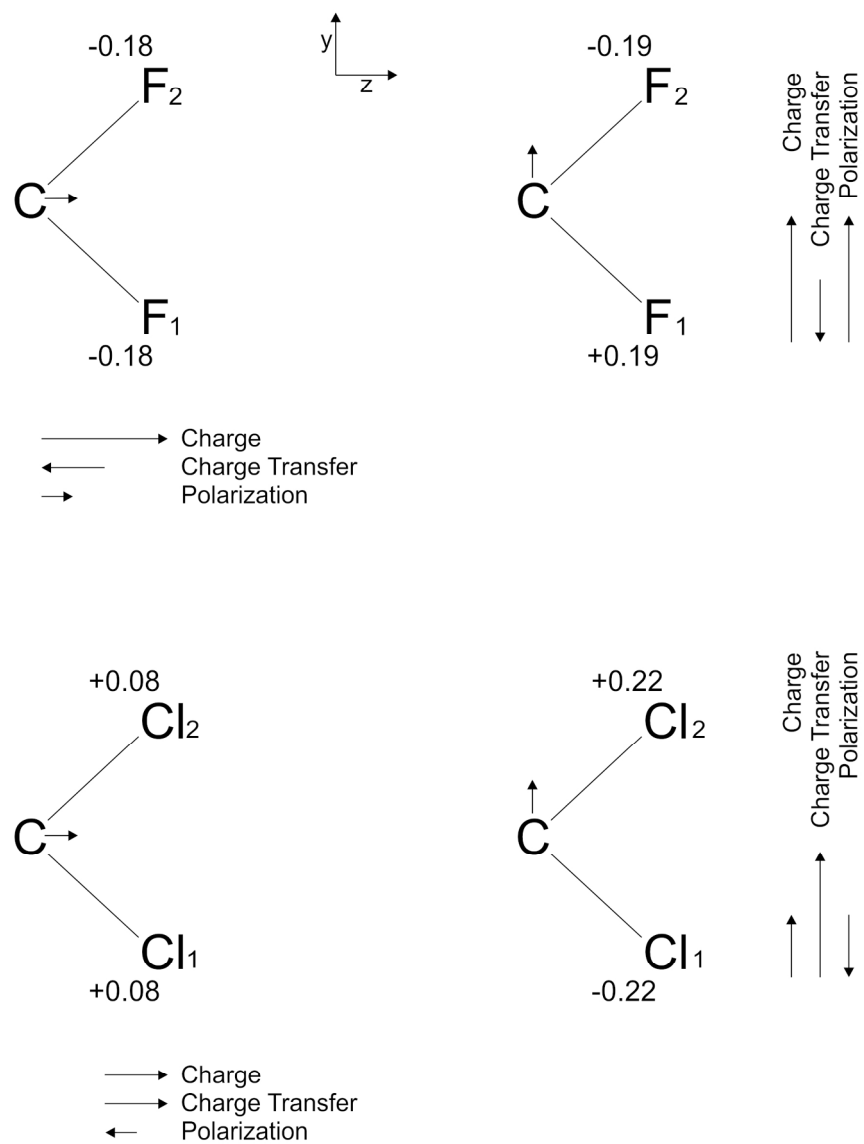


Figure 2. QTAIM charge, charge transfer and polarization contributions for the dynamic carbon contribution for the symmetric and asymmetric stretching intensities of  $\text{CH}_2\text{F}_2$  and  $\text{CH}_2\text{Cl}_2$ . The numbers given for the atoms are values of the charge transfer derivatives owing to the carbon atom displacements.  
159x208mm (300 x 300 DPI)

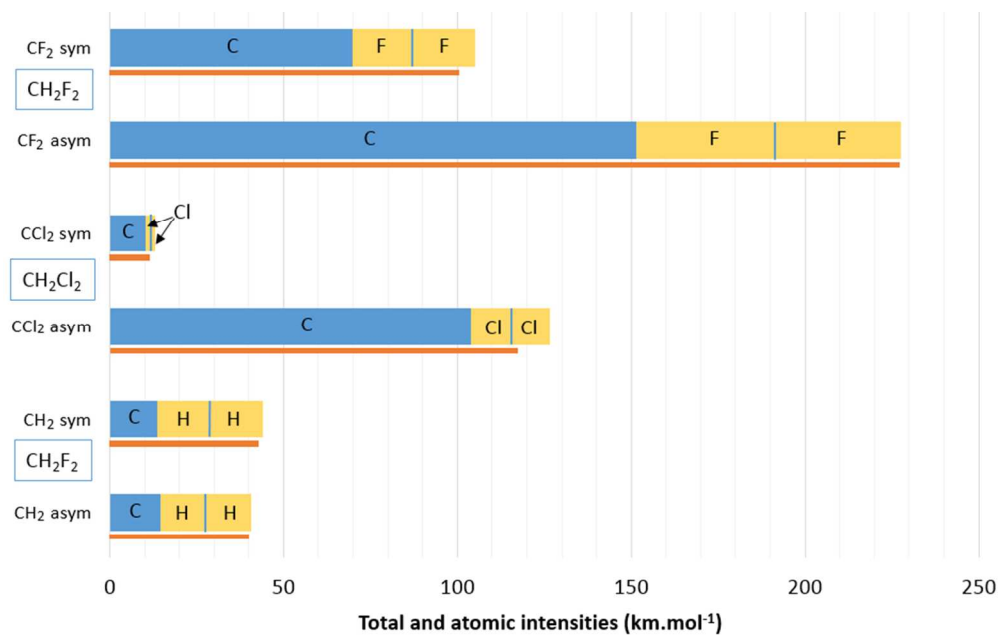


Figure 3. Bar graphs showing the dynamic atomic contributions for the symmetric and asymmetric CF, CCl and CH stretches of CH<sub>2</sub>F<sub>2</sub> and CH<sub>2</sub>Cl<sub>2</sub>. The thin bars below the dynamic atomic contributions represent the total infrared intensities.  
248x155mm (96 x 96 DPI)

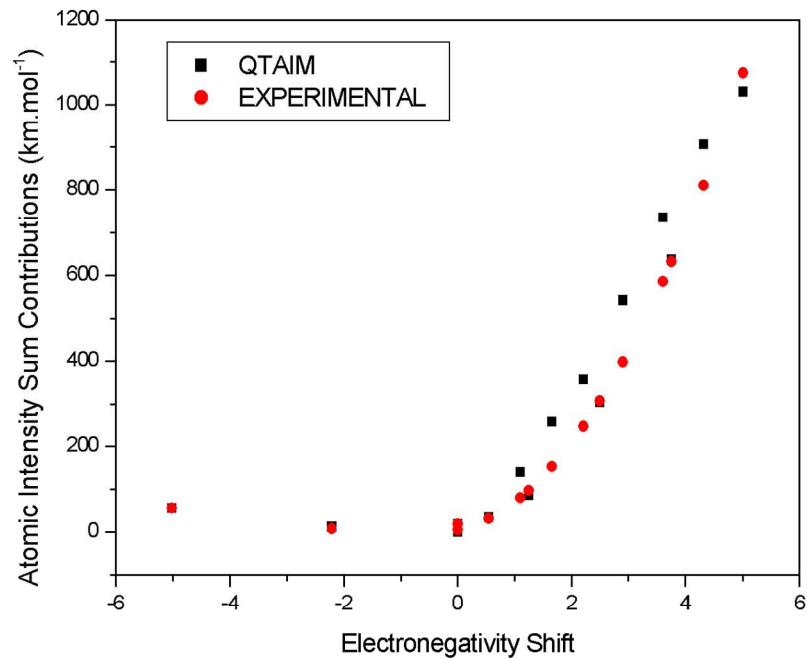


Figure 4. Atomic intensity sum contributions determined from the QAIM calculations and from the electronegativity model vs. the relative electronegativities of the fluorochloromethane atoms.  
279x215mm (150 x 150 DPI)

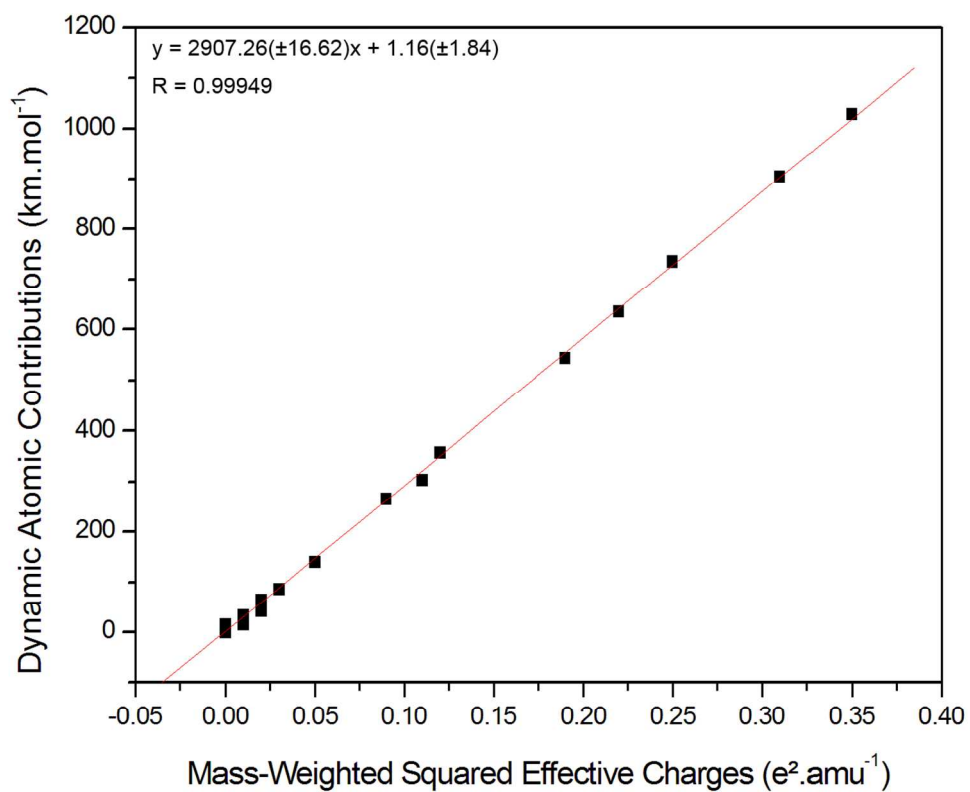


Figure 5. Graph of the dynamic atomic intensity contributions of the fluorochloromethane atoms determined from QCISD/cc-pVTZ calculations against the mass-weighted squared effective charges determined from polar tensors at the same quantum level.

370x311mm (96 x 96 DPI)